Depolymerization of Phospholamban in the Presence of Calcium Pump: A Fluorescence Energy Transfer Study†

Laxma G. Reddy,‡ Larry R. Jones,§ and David D. Thomas*,‡

Department of Biochemistry, University of Minnesota Medical School, Minneapolis, Minnesota 55455, and Krannert Institute of Cardiology, Indiana University, Indianapolis, Indiana 46202

Received July 24, 1998; Revised Manuscript Received December 15, 1998

ABSTRACT: Phospholamban (PLB), a 52-amino acid protein, regulates the Ca-ATPase (calcium pump) in cardiac sarcoplasmic reticulum (SR) through PLB phosphorylation mediated by β-adrenergic stimulation. The mobility of PLB on SDS−PAGE indicates a homopentamer, and it has been proposed that the pentameric structure of PLB is important for its regulatory function. However, the oligomeric structure of PLB must be determined in its native milieu, a lipid bilayer containing the Ca-ATPase. Here we have used fluorescence energy transfer (FET) to study the oligomeric structure of PLB in SDS and dioleoylphosphatidylcholine (DOPC) lipid bilayers reconstituted in the absence and presence of Ca-ATPase. PLB was labeled, specifically at Lys 3 in the cytoplasmic domain, with amine-reactive fluorescent donor/acceptor pairs. FET between donor- and acceptor-labeled subunits of PLB in SDS solution and DOPC lipid bilayers indicated the presence of PLB oligomers. The dependence of FET efficiency on the fraction of acceptor-labeled PLB in DOPC bilayers indicated that it is predominantly an oligomer having 9−11 subunits, with ~10% of the PLB as monomer, and the distance between dyes on adjacent PLB subunits is 0.9 ± 0.1 nm. When labeled PLB was reconstituted with purified Ca-ATPase, FET indicated the depolymerization of PLB into smaller oligomers having an average of 5 subunits, with a concomitant increase in the fraction of monomer to 30−40% and a doubling of the intersubunit distance. We conclude that PLB exists primarily as an oligomer in membranes, and the Ca-ATPase affects the structure of this oligomer, but the Ca-ATPase binds preferentially to the monomer and/or small oligomers. These results suggest that the active inhibitory species of PLB is a monomer or an oligomer having fewer than 5 subunits.

In cardiac muscle, the Ca-ATPase activity of sarcoplasmic reticulum (SR)[1] is modulated by a small membrane protein, phospholamban (PLB), in a phosphorylation-dependent manner. In its unphosphorylated state, PLB inhibits the Ca-ATPase at submicromolar Ca concentrations. This inhibition is relieved upon PLB phosphorylation by either cAMP-dependent protein kinase or Ca/calmodulin-dependent protein kinase II (*1*−*3*). This regulation of the Ca-ATPase through PLB phosphorylation is proposed to be the underlying mechanism for β-adrenergic stimulation of the heart (*4*−*6*). Even though the regulatory role of PLB in cardiac SR is well-established at the functional level, the underlying physical mechanism of this regulation is not clear. Sodium dodecyl sulfate−polyacrylamide gel electrophoresis (SDS−PAGE) and low-angle laser light scattering in SDS solutions (*7*, *8*) showed that PLB is a homopentamer in equilibrium with a small fraction of monomer. The oligomeric state of PLB has been proposed to play an important role in the mechanism of Ca-ATPase regulation (*1*, *2*, *9*−*11*). Based on systematic substitutions of amino acids and their effects on the stability of the PLB pentamer on SDS−PAGE, a model for a tightly packed coiled-coil pentamer (*9*, *12*) has been proposed: the α-helical transmembrane domains of five monomers associate by intramembrane Leu/Ile interactions forming a Leu/Ile zipper (*9*, *13*). Substitution of Ala for specific Leu or Ile residues, proposed to be involved in the formation of the zipper, was shown to form monomers on SDS−PAGE and to potentiate the inhibitory activity of PLB (*14*, *15*). These results led to the hypothesis that the monomeric form of PLB may be the active inhibitory species. However, the oligomeric structure of PLB in SDS is not necessarily the same as in the native membrane environment. This necessitates the study of the quaternary structure of PLB in a lipid bilayer, in the absence and presence of the Ca-ATPase.

† This work was supported by grants to D.D.T. from the National Institutes of Health (GM27906, AR32961) and the Minnesota Supercomputer Institute. L.G.R. was supported by a grant from the American Heart Association, National Center. L.R.J. was supported by grants (HL06308 and HL49428) from the National Institutes of Health.

* To whom correspondence should be addressed.

‡ University of Minnesota Medical School.

§ Indiana University.

[1] Abbreviations: FET, fluoresence energy transfer; PLB, phospholamban; SR, sarcoplasmic reticulum; PKA, cAMP-dependent protein kinase; Cam kinase, calcium/calmodulin-dependent protein kinase; Dansyl, 2-(dimethylamino)naphthalene-6-sulfonyl; DABSYL, 4-(dimethylamino)benzene-4′-sulfonyl; ASE, *N*-methylanthranilate succinimido ester; DABCYL, 4-[[4-(dimethylamino)phenyl]azo]benzoic acid; SDS, sodium dodecyl sulfate; $C_{12}E_8$, octaethylene glycol monododecyl ether; β-OG, β-octyl glucoside; DOPC, dioleoylphosphatidylcholine; DOPE, dioleoylphosphatidylethanolamine; HRP, horseradish peroxidase; DAB, 3,3′-diaminobenzidine tetrahydrochloride; NAc-Lys-NMe, *N*α-acetyllysine carboxymethylamide; NAc-Cys, *N*α-acetylcysteine; NAc-Tyr-NH_2, *N*α-acetyltyrosine carboxylamide; DTT, dithiothreitol; TFE, trifluoroethanol; MOPS, 3-(*N*-morpholino)propanesulfonic acid; SDS−PAGE, sodium dodecyl sulfate−polyacrylamide gel electrophoresis; EPR, electron paramagnetic resonance; PVDF, polyvinylidene difluoride; TLC, thin-layer chromatography; DMF, dimethylformamide.

10.1021/bi981795d CCC: $18.00
Published on Web 00/00/0000 PAGE EST: 8.3

The first study to measure the oligomeric state of PLB in lipid bilayers, using EPR spectroscopy, showed that PLB exists in an average oligomeric size of 3.5 in DOPC vesicles, and upon phosphorylation the oligomeric size increases to 5.3 (*16*). This study suggested the existence of a dynamic equilibrium between PLB subunits in the lipid bilayer and that the regulation of PLB's oligomeric state is critical for its regulation of the Ca-ATPase (*11*). However, that method is useful only for measuring the average oligomeric structure and cannot resolve the relative distribution of oligomeric and monomeric species. Also, since the EPR method used spin-labeled lipid to measure the number of boundary lipids in contact with protein, and since the Ca-ATPase is much larger than PLB, the method cannot be used reliably to determine specifically the oligomeric state of PLB in the presence of the Ca-ATPase. In the present study, we have used fluorescence energy transfer (FET) to measure the oligomeric state of dye-labeled, purified recombinant PLB in SDS and DOPC bilayers reconstituted in the absence and presence of purified Ca-ATPase. Since the dyes are attached specifically to PLB, the oligomeric state can be measured just as reliably in the presence or absence of the Ca-ATPase.

MATERIALS AND METHODS

Reagents. The amino-reactive dyes, 2-(dimethylamino)-naphthalene-6-sulfonyl chloride (dansyl chloride), 4-(dimethylamino)benzene-4′-sulfonyl chloride (DABSYL chloride), *N*-methylanthranilate (ASE), and 4-[[4-(dimethylamino)phenyl]azo]benzoic acid (DABCYL) succinimido esters were purchased from Molecular Probes (Eugene, OR). Sodium dodecyl sulfate (SDS), octaethylene glycol monododecyl ether ($C_{12}E_8$), and β-octyl glucoside (β-OG) were purchased from Calbiochem (San Diego, CA). Dioleoylphosphatidylcholine (DOPC) and dioleoylphosphatidylethanolamine (DOPE) were purchased from Avanti Polar Lipids (Alabaster, AL). The reagents for SDS−PAGE (16.5% polyacrylamide Tris−tricine ready gels and the Tris−tricine gel running buffer), Biobeads SM2, and the PVDF membrane used for immunoblots were purchased from Bio-Rad Laboratories (Richmond, CA). Anti-PLB monoclonal antibody (2D12) is described in ref *13*. Centricon filters were procured from Amicon, Inc., (Beverly, MA). Horseradish peroxidase (HRP) coupled goat anti-mouse antibody was purchased from Fisher (Southern Biotechnology Laboratories, Inc.). The substrate for HRP, 3,3′-diaminobenzidine tetrahydrochloride (DAB) reagent, was purchased from Sigma (St. Louis, MO).

Sample Preparation. Recombinant phospholamban was expressed in Sf21 insect cells after infection with baculovirus and purified by monoclonal antibody (2D12) affinity column chromatography, as previously described (*9*, *17*). The concentration of PLB was determined by the amido black assay (*18*). The purified protein was stored at −70 °C at a protein concentration of 1.5−2.5 mg/mL, in a buffer containing 88 mM MOPS, 18 mM glycine, 5 mM DTT, and 0.92% β-octyl glucoside (β-OG) at pH 7.2. Rabbit skeletal sarcoplasmic reticulum (SR) Ca-ATPase was purified from light SR by reactive red affinity chromatography (*19*).

Labeling PLB with Fluorescent Dyes. Recombinant PLB expressed in insect cells was purified in a buffer containing 88 mM MOPS, 18 mM glycine, 5 mM DTT, and 0.92% β-octyl glucoside (β-OG) at pH 7.2. It was essential to remove the glycine before labeling, to prevent its reaction with the amino-specific dyes. An aliquot of PLB was diluted to 1.5 mL with labeling buffer (0.1 M $NaHCO_3$ containing 0.01% $C_{12}E_8$, pH 8.3) and centrifuged at 5000 rpm (SS 34 rotor, Sorvall) in Centricon tubes, with Centricon 3 filters (3000 MW cutoff), until the volume was reduced to 0.2 mL. Dilution of the sample to 1.5 mL and centrifugation until the sample volume was reduced to 0.2 mL was repeated 6 times to lower the concentration of glycine to at least 100 times less than that of PLB.

We have tested sulfonyl chlorides of dansyl and DABSYL and succinimido esters of ASE and DABCYL, in an attempt to label specifically the ϵ-amino group of the single Lys (residue 3) present in PLB. Since these dyes are also known to react with side chains of Cys and Tyr, we tested their reactivity using individual amino acid derivatives *N*-acetyllysine carboxylamide, *N*-acetyltyrosine carboxylamide, and *N*-acetylcysteine under the conditions used to label PLB. The reactivity of the dyes with the amino acids was tested by TLC (Whatman, silica gel 150A K5) in 10−20% methanol in $CHCl_3$ as solvent (mobile phase). Although these dyes were found to react with all three of these amino acids, 10 mM either hydroxylamine, β-mercaptoethanol, or DTT was able to reverse the side-chain labeling of Cys and Tyr by succinimido esters but not by sulfonyl chlorides (shown by TLC). The labeling of the Lys side chain by either succinimido esters or sulfonyl chlorides was not reversible under similar conditions. Thus, employing the following procedure, we have used succinimido esters of ASE and DABCYL to label PLB specifically at Lys 3.

The washed PLB (∼75−100 μM) was labeled in 0.1 M $NaHCO_3$ containing 0.01% $C_{12}E_8$ by adding the dye from DMF stock solutions at a molar ratio of dye/PLB = 10 and incubating at room-temperature overnight (12−16 h). The final concentration of DMF in the labeling mixture was < 5%. More than 5% solvent in the reaction mixture caused the aggregation of labeled PLB into very large oligomers on SDS−PAGE. The unreacted label was removed by washing the PLB/dye sample three times (1.5 mL each) with 0.1 M $NaHCO_3$ containing 0.01% $C_{12}E_8$, using Centricon-3 filters (3000 MW cutoff). Then the sample was incubated with 10 mM DTT in 20 mM MOPS (pH 7.0), to remove potential nonspecific labeling of Tyr and Cys, followed by three more washes with 20 mM MOPS (pH 7.0) containing 0.01% $C_{12}E_8$. Concentration of PLB in the final sample was measured by the amido black method (*18*), and the dye stoichiometry was measured spectrophotometrically using the extinction coefficients of the dye−*N*ϵ-acetyl-Lys-CONHMe (λ_{330} = 3500 M^{-1} cm^{-1} for ASE conjugates and λ_{445} = 37 000 M^{-1} cm^{-1} for DABCYL conjugates). The final dye/PLB ratio was in the range of 0.9−1.2 for succinimido ester dyes, consistent with specific labeling of the single Lys residue of PLB at position 3.

Ca-ATPase/PLB Coreconstitution and Functional Studies. The method used for functional reconstitution of Ca-ATPase and labeled PLB has been described previously (*17*, *20*) adopted from Levy et al. (*21*−*23*): In short, 11 μg of labeled PLB was dried and solubilized in 80 μL of $CHCl_3$ containing 0.8 mg of DOPC/DOPE (DOPC/DOPE = 4, by weight) and 20 μL of TFE. The solvent was dried under nitrogen, and the residual solvent was removed by pumping the sample

under vacuum. The dried lipid/PLB film was hydrated with 50 μL of 20 mM imidazole (pH 7.0) by vortexing thoroughly, followed by sonication for 1 min (bath-type sonicator with single power output setting, Laboratory Supplies Company, Inc., Hicksville, NY). The resulting PLB/lipid vesicles were adjusted to final concentrations of 20 mM imidazole (pH 7.0), 0.1 M KCl, 5 mM $MgCl_2$, 10% glycerol, 1.6 mg of β-OG, followed by the addition of 20 μg of purified Ca-ATPase (5 mg/mL stock in 20 mM MOPS, pH 7.0, 1.0 mM $CaCl_2$, 1.0 mM $MgCl_2$, 0.25 mM DTT, 20% glycerol, 0.1% $C_{12}E_8$, and 2.5 mg/mL DOPC), and the final volume was adjusted to 100 μL. The detergent was then removed by incubation with 40 mg of Biobeads for 3 h at room temperature. The resultant Ca-ATPase/PLB lipid vesicles were separated from Biobeads by pipeting the vesicles with a narrow tip (used for loading sample on SDS−PAGE) and assayed for Ca-ATPase function immediately by measuring the Ca-dependent release of inorganic phosphate from ATP, using the method of Lanzetta et al. (*24*). Prior to the assay, the reconstituted vesicles were incubated with PLB antibody (+antibody) at a PLB/PLB antibody molar ratio of 1.0 or the antibody buffer (−antibody) for 15 min on ice.

Reconstitution of PLB into Lipid Bilayers for FET. Two methods of reconstitution were used to incorporate the labeled PLB into DOPC lipid bilayers for FET studies. Method I provided a more direct comparison with previous spectroscopic studies, while method II provided a more direct comparison with functional measurement in the present study and previous studies.

Method I. This method is similar to the method of Cornea et al. (*16*). Labeled PLB (2.16 μg or 0.36 nmol) at various mole fractions of acceptor (P_A) in 20 μL of 20 mM MOPS, pH 7.0, and ~0.01% $C_{12}E_8$ was added to a dried DOPC lipid film (the molar ratio of lipid/PLB = 100−120). The mixture was incubated for 1 h at room temperature with frequent vortexing. Then 100 μL of 20 mM MOPS (pH 7.0), 0.1 M KCl, and 5 mM $MgCl_2$ (MOPS buffer) was added, followed by sonication for 1 min as above. The samples were then diluted to 1.0 mL with MOPS buffer and centrifuged at 100 000 rpm (Beckman, TL100.2) for 2 h. The resulting pellet was resuspended in 0.12 mL of MOPS buffer, in which the final concentration of total PLB was at 3.0 μM.

For coreconstitution, purified skeletal SR Ca-ATPase (5 mg/mL stock) in elution buffer (20 mM MOPS, pH 7.0, 1.0 mM $CaCl_2$, 1.0 mM $MgCl_2$, 0.25 mM DTT, 20% glycerol, 0.1% $C_{12}E_8$ and 2.5 mg/mL DOPC) was added to PLB/DOPC (2.16 μg or 0.36 nmol of PLB and the molar ratio of lipid/PLB = 120) vesicles after the sonication step (see above, before dilution and centrifugation) to give the required PLB/Ca-ATPase ratios, and the vesicles were incubated on ice for another 2 h. To the samples with high PLB/Ca-ATPase ratios (more than a PLB/Ca-ATPase molar ratio of 0.5), which received less volume of Ca-ATPase stock, and the samples containing no Ca-ATPase, elution buffer (in which Ca-ATPase was purified) was added to compensate for the volume of the Ca-ATPase stock (e.g., at a molar ratio of PLB/Ca-ATPase = 0.5, the volume of purified Ca-ATPase stock added was 14 μL, the elution buffer added to no Ca-ATPase sample was 14 μL, and all other samples received Ca-ATPase stock and elution buffer to total 14 μL). Then the sample was diluted to 1.0 mL with MOPS buffer and centrifuged at 100 000 rpm (Beckman, TL100.2) for 2 h. The resulting pellet was resuspended in 0.12 mL of MOPS buffer. The supernatant was dried and resuspended in SDS−PAGE sample buffer for immunoblot analysis: no PLB was detected on the immunoblots, indicating no loss of PLB during centrifugation. Thus the final PLB concentration was 3.0 μM.

Method II. This method is similar to the one described previously by Reddy and others in demonstrating the functional coreconstitution of the Ca-ATPase with PLB (*17*, *21*−*23*). To a dried sample of 2.16 μg or 0.36 nmol of labeled PLB (in 20 mM MOPS, pH 7.0, and 0.01% $C_{12}E_8$) was added DOPC (molar ratio of lipid/PLB = 120) in 80−100 μL of $CHCl_3$, and PLB was solubilized by adding ~20 μL of TFE (sample becomes clear after the addition of TFE). After the removal of solvent under nitrogen, the contents were further dried under vacuum. The dried lipid/PLB/$C_{12}E_8$ was resuspended in 50 μL of MOPS buffer by vortexing, followed by sonication for 1 min (bath-type sonicator as above).

For coreconstitution, after the sonication of labeled PLB in DOPC, purified skeletal SR Ca-ATPase (5 mg/mL stock) in elution buffer (20 mM MOPS, pH 7.0, 1.0 mM $CaCl_2$, 1.0 mM $MgCl_2$, 0.25 mM DTT, 20% glycerol, 0.1% $C_{12}E_8$, and 2.5 mg/mL DOPC) was added to the sample to give the desired PLB/Ca-ATPase ratio, as described in method I, and incubated on ice for another 2 h. The final volume was adjusted to 0.12 mL with MOPS buffer without $C_{12}E_8$. The detergent was removed by incubating the sample with Biobeads SM2 (~1 mg) for 3 h at room temperature, followed by the removal of Biobeads by pipeting the PLB/Ca-ATPase vesicles with a narrow pipet tip.

Calculation of Quantum Yield (ϕ) and R_0. The fluorescence quantum yield was determined by comparing the integrated intensity of the corrected emission spectrum of an unknown with that of a sample having a known fluorescence quantum yield (*25*), normalizing to the sample's absorbance and the excitation intensity. The quantum yield of the donor fluorophore (ASE) was measured from ASE-labeled PLB, using as a standard 1-(dimethylamino)naphthalene-5-sulfonate (DNS) in 0.1 M $NaHCO_3$, which is known to have a quantum yield of 0.36 (*25*). R_0 was calculated according to (*26*)

$$R_0 = (9.7 \times 10^3)(J\,\kappa^2 n^{-4}\Phi_D)^{1/6}$$

where J is a measure of spectral overlap between donor emission and acceptor absorption; κ is a geometric factor that depends on the relative orientation of donor and acceptor (assigned the value $^2/_3$, assuming random orientation of both donor and acceptor on the fluorescence time scale), n is the refractive index of the medium (1.33, as normally used for aqueous medium), and Φ_D is the quantum yield of the donor fluorophore. The spectral overlap (J) was calculated according to

$$J = \int_0^\infty F_d(\lambda)\epsilon_a(\lambda)\lambda^4\,d\lambda$$

where F_d is the normalized fluorescence of the donor and ϵ_a is the extinction coefficient of the acceptor.

Fluorescence Energy Transfer Measurements. Donor- and acceptor-labeled PLB were mixed at various molar fractions of acceptor (P_a) (a) in SDS−PAGE gel running buffer containing 0.1% SDS, 0.025 M Tris, and 0.193 M glycine

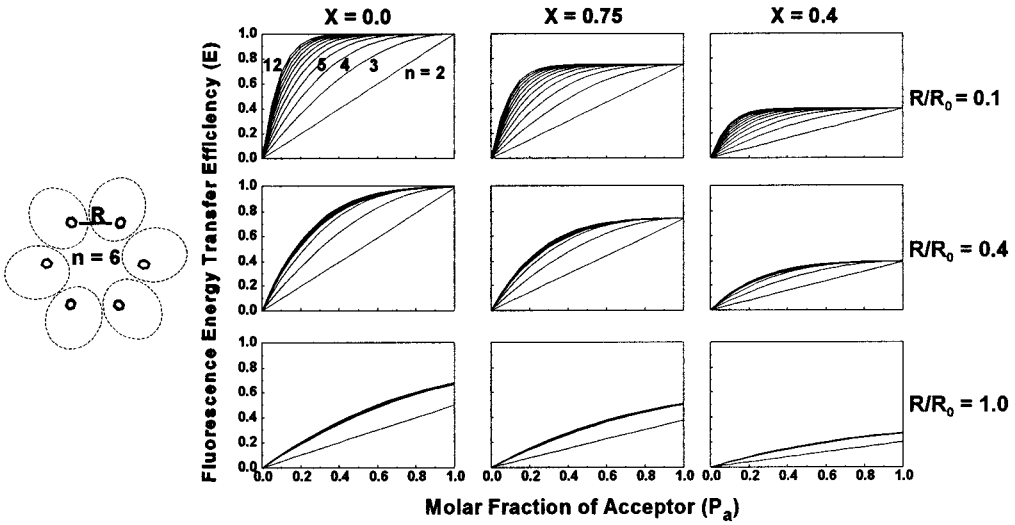

FIGURE 1: Simulated fluorescence energy transfer within a two-dimensional symmetric ring (left), in which *n* is the number of subunits within the oligomer, *R* is the distance between chromophore sites on adjacent subunits, and *X* is the molar fraction of subunits that are monomeric (*27*). All subunits are labeled randomly with either donor or acceptor. Plots show the predicted sensitivity of the observed energy transfer efficiency (*E*) on these variables.

(SDS buffer); (b) in 0.1% $C_{12}E_8$, 20 mM MOPS, pH 7.0, and 0.1 M KCl; or (c) by reconstituting in DOPC lipid vesicles suspended in 20 mM MOPS, pH 7.0, 0.1 M KCl, and 5 mM $MgCl_2$ (MOPS buffer). In SDS and $C_{12}E_8$, the FET measurements were made before and after incubating the sample at 100 °C for 5 min. All spectroscopic measurements were performed at a temperature of 25 ± 1 °C.

Steady-state fluorescence emission spectra were recorded on a SPEX-Fluorolog II spectrofluorometer (Edison, NJ) in a 3 mm × 3 mm quartz cuvette, with excitation at 330 nm. Excitation and emission bandwidths were set at 7 and 10 nm, respectively. The emission spectrum (from 300 to 550 nm) was obtained with a step size of 1 nm and an integration time of 1.0 s/step. Each fluorescence spectrum was corrected by subtracting a corresponding buffer blank lacking PLB, and the intensity was corrected for the sensitivity of the detector, using a standard lamp. Light scattering had no effect on the spectrum, as verified by scanning the emission near the excitation wavelength. The peak value of the emission spectrum was taken as the fluorescence intensity for calculation of the energy transfer efficiency, $E = 1 - F_{DA}/F_D$, where F_{DA} is the fluorescence of donor in the presence of acceptor (normalized by donor concentration) and F_D is the fluorescence of donor in the absence of acceptor.

Analysis of Fluorescence Data. The fluorescence energy transfer data were analyzed by assuming that the PLB molecules were in symmetric ring-shaped oligomers having *n* subunits, plus a monomeric molar fraction *X*, and intersubunit distance *R*, following the method of theoretical simulation and fitting developed by Li et al. (*27*), as illustrated in Figure 1. All subunits were assumed to be labeled with either donor or acceptor (molar fraction P_a) and randomly mixed. This analysis assumes a specific oligomeric structure in equilibrium with a monomeric fraction, with negligible intermediate oligomeric forms. This assumption is not easily testable by this method, but it is consistent with the behavior of PLB on SDS−PAGE (*9*), and it is consistent with typical behavior of oligomeric protein complexes. The energy transfer efficiency was assumed to be negligible for donors on monmeric subunits, as verified in similar experiments on monomeric mutants of PLB (*27*). The lack of energy transfer for monomeric donors is consistent with the density of PLB in the membranes, 1 PLB per 120 lipids, indicating that the average separation between PLB protomers is at least on the order of 11 lipid molecules, or about 100 Å, which is more than a factor of 2 greater than R_0. Li et al. (*27*) showed that a plot of *E* vs P_a (Figure 1) can be used to determine independently the variables *R*, *n*, and *X*, by fitting experimental data sets to the simulated curves. The plots in Figure 1 show that the monomeric fraction *X* can be determined from the asymptotic value of $(1 - E)$ as P_a approaches 1. Curvature in the plots is observed only if $n > 2$ and is particularly sensitive to *n* if R/R_0 is much less than 1, which is likely to be true in the case of small protein subunits such as PLB (*27*). Data were analyzed by fitting the data (plot of *E* vs P_a) to simulated curves (Figure 1), varying the three parameters (*R*, *n*, and *X*) until a best fit (minimum χ^2) was obtained (*27*).

RESULTS

Labeling Specificity, Stoichiometry, and Characterization. Labeling PLB with sulfonyl chlorides of dansyl and DABSYL yielded a dye/PLB molar ratio of 1.8−2.2, indicating poor specificity of labeling at Lys 3. We tested these sulfonyl chloride derivatives and also succinimido ester derivatives of ASE and DABCYL, by reacting them with *N*-acetyllysine carboxylamide (Lys side chain), *N*-acetyltyrosine carboxylamide (Tyr side chain), and *N*-acetylcysteine (Cys side chain). Under the conditions of PLB labeling, all three side chains showed similar reactivity with sulfonyl chlorides, while the Lys side chain was the most reactive of the three with succinimido esters (Figure 2). Incubation of all three amino acids with succinimido esters indicated that Lys reacted almost completely in 1 h while unreacted Tyr and Cys were detected by ninhydrin reagent on TLC, even after overnight incubation. Incubation with 10 mM DTT, β-mercaptoethanol, or hydroxylamine for 60 min at 25 °C cleaved the succinimido derivative dye from Tyr and Cys side chains (Figure 2, compare lanes 3 and 4 of panels B and C) but not from the Lys side chain and cleaved sulfonyl derivative dyes

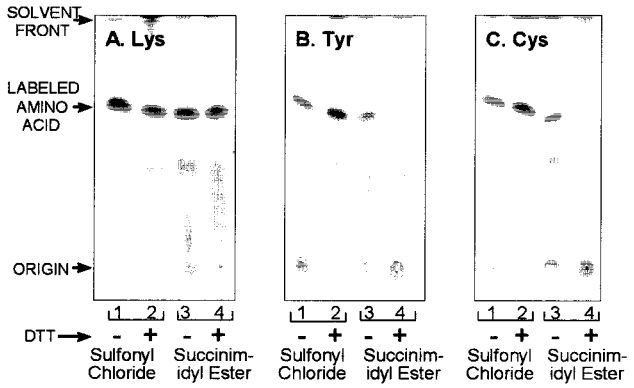

FIGURE 2: Reactivity of Lys, Tyr, and Cys side chains with sulfonyl chloride derivative of DABSYL and succinimido ester derivative of DABCYL. The reversibility by DTT of the succinimido reaction with Tyr and Cys is also shown. The spots were visualized by the intense red color of the DABSYL or DABCYL dye. Ninhydrin test indicated the presence of unreacted amino acid at the origin (not shown here). Unreacted dye migrates as a streak from the origin to the middle of the plate. TLC was performed on silica gel-coated glass plates, and 20% methanol in $CHCl_3$ was used as solvent.

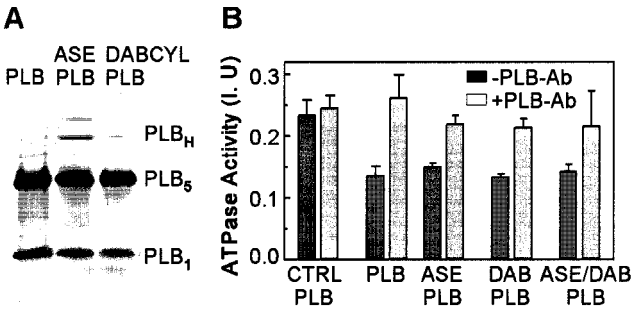

FIGURE 3: (A) SDS−PAGE/immunoblot of unlabeled (native), donor-labeled (ASE), and acceptor-labeled (DABCYL) PLB. PLB_1 = monomer, PLB_5 = pentamer, PLB_H = higher oligomer. (B) Inhibitory effects of donor- and acceptor-labeled PLB measured at 25 °C in a medium containing 50 mM imidazole, pH 7.0, 0.1 M KCl, 5 mM $MgCl_2$, 0.158 μM free Ca^{2+}(pCa 6.8), and 1 μg/mL calcium ionophore (A23187). The assay was started by adding 2.5 mM ATP. + PLB-Ab indicates that the molar ratio of anti-PLB antibody to PLB was 1.0, which is sufficient for saturation (*17*, *20*). The values presented are mean ± SEM (n = 3).

from all three amino acid side chains. Even after longer (up to 24 h) incubation with DTT, there was no significant reversal of the reactions of (a) the sulfonyl chlorides with any of the three amino acids and (b) the succinimido esters with Lys. We used the same method of PLB labeling with ASE or DABCYL succinimido esters, followed by the DTT treatment, resulting in a final labeling ratio of 1.0−1.2 dye/PLB, strongly suggesting the specific labeling of Lys 3.

On SDS−PAGE, the dye-labeled PLB samples showed the same monomer and pentamer pattern as exhibited by unlabeled PLB, except for a minor PLB component present in ASE-labeled samples, the apparent molecular weight of which corresponds roughly to that of an octamer to decamer (PLB_H, Figure 3A). The inhibitory function of labeled PLB was tested in lipid vesicles by coreconstitution with Ca-ATPase purified from skeletal SR. The inhibition induced by either ASE- or DABCYL-labeled PLB was comparable to that of unlabeled PLB, and the inhibition was reversed by the anti-PLB monoclonal antibody 2D12 as reported previously (*17*, *20*) (Figure 3B). The method used for the functional studies is similar to method II used for the

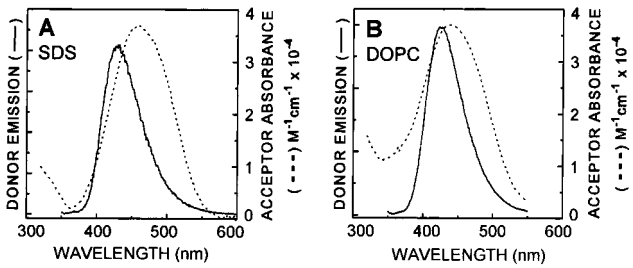

FIGURE 4: Spectral overlap of donor fluorescence and acceptor absorption. Fluorescence emission spectrum of ASE-PLB (—) and absorption spectrum of DABCYL-PLB (- - -) in SDS (A) and in DOPC vesicles (B).

coreconstitution of PLB/Ca-ATPase for FET studies. It has been shown that the orientation of Ca-ATPase is right-side-out in this type of preparation (*21*−*23*). However, our unpublished results (accessibility to trypsin and PKA phosphorylation) indicate that the orientation of PLB is symmetric (bidirectional).

R_0 Calculation. The emission and absorption spectra of the donor- and acceptor-labeled PLB in SDS and DOPC are shown in Figure 4. The calculated quantum yield for donor-labeled PLB was 0.44 ± 0.05 in SDS and 0.37 ± 0.02 in DOPC. The spectral overlap was high for the ASE/DABCYL pair, and the calculated R_0 was 46.1 ± 0.8 Å in SDS and 42.2 ± 0.4 Å in DOPC.

FET of PLB in SDS, DOPC Bilayers, and $C_{12}E_8$. Desired ratios of donor-labeled PLB and acceptor-labeled PLB, in separate $C_{12}E_8$ stock solutions, were (a) added directly to a detergent solution or (b) premixed in $C_{12}E_8$ and reconstituted into DOPC bilayers. The total PLB concentration, and the ratio of PLB to detergent or lipid, was independent of the acceptor/donor ratio. In most experiments, all PLB molecules were labeled with either donor or acceptor. Alternatively, we measured FET at a fixed concentration of donor (10% of the total PLB), keeping the final concentration of PLB constant by adding corresponding amounts of unlabeled PLB, with no significant change in the results.

The fluorescence energy transfer efficiency E was measured as a function of the molar fraction of acceptor, P_a. In SDS, no energy transfer was observed, even when the sample was incubated for up to 24 h at room temperature, unless the sample was boiled (for 5 min and then equilibrated for 30 min at room temperature) before fluorescence was measured (Figure 5). Boiling the sample for longer than 5 min had no further effect on the transfer efficiency. It is well-known that boiling PLB disrupts pentamers, which spontaneously reaggregate at lower temperatures (*1*). In contrast, when donor/acceptor-PLB were reconstituted from detergent solution into DOPC bilayers, significant energy transfer was observed (Figure 5), and this was not affected by boiling the mixed sample in detergent before reconstitution. In lipids, no further effect on energy transfer efficiency was observed when samples were treated with sonication, boiling, and several freeze/thaw cycles. Therefore, we conclude that the mixing of donor- and acceptor-labeled PLB was complete in DOPC.

Figure 5 shows the best fits of the data to the model illustrated in Figure 1, a ring-shaped oligomer with n subunits, a monomeric molar fraction X, and an intersubunit distance R. Even before quantitative fitting, a comparison

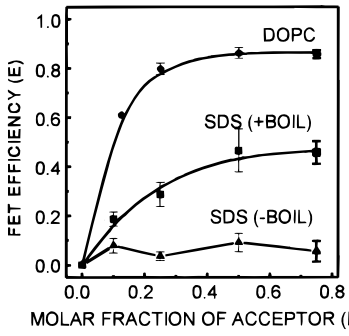

FIGURE 5: Fluorescence energy transfer (FET) efficiency (E) between donor- and acceptor-labeled PLB, as a function of molar fraction of acceptor (P_a): In SDS, before (▲) and after (■) boiling and in DOPC vesicles (●). PLB was reconstituted in DOPC vesicles according to method I. The smooth curves are fits to the experimental data (symbols), mean ± SEM ($n \geq 3$).

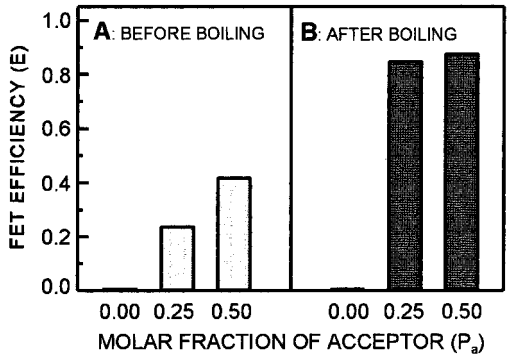

FIGURE 6: Effect of boiling on FET efficiency of donor- and acceptor-labeled PLB in $C_{12}E_8$. The results are an average of two experiments.

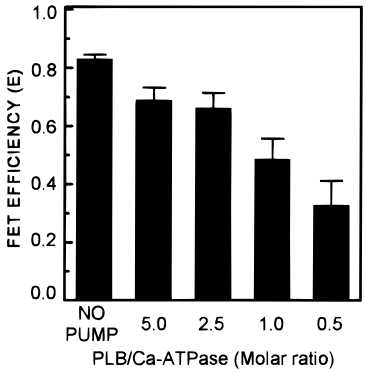

FIGURE 7: Fluorescence energy transfer between PLB subunits, at $P_a = 0.50$, as a function of the molar ratio of Ca-ATPase to PLB. Coreconstitution in DOPC vesicles was done according to method I. The results represent mean ± SEM ($n = 3$).

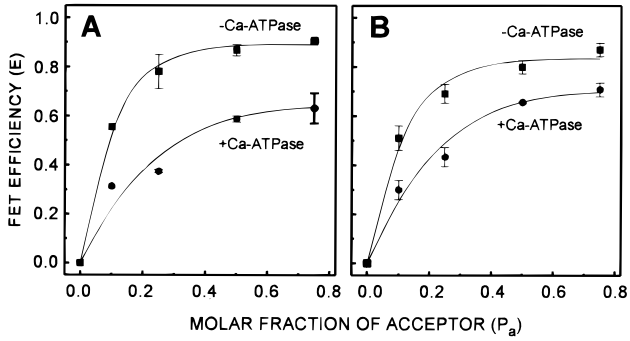

FIGURE 8: FET efficiency vs molar fraction of acceptor in ASE (donor) and DABCYL (acceptor) labeled PLB reconstituted in the absence (■) and presence (●) of purified Ca-ATPase in DOPC according to method I (A) and method II (B). The smooth curves are fits to the experimental data (symbols), mean ± SEM ($n = 3$).

of the data with the simulations in Figure 1 shows clearly that both in SDS (after boiling) and DOPC, the samples are primarily oligomeric. The high degree of curvature, particularly in DOPC, indicates that the oligomer size n is large; and the high E value reached at high acceptor levels, particularly in DOPC, indicates that the monomeric fraction X is small. In SDS, the FET data is best fit to an oligomer, $n = 5-7$, with 53.7% ± 5.0% monomer and an intersubunit distance $R = 22.0 \pm 2.7$ Å. In DOPC, the oligomeric size is larger ($n = 9-11$), the monomeric fraction is smaller ($X = 12.8 \pm 2.0\%$), and the intersubunit distance is smaller ($R = 8.9 \pm 0.6$ Å). The uncertainties are SEM ($n = 3$).

In $C_{12}E_8$, the FET efficiency was significant before boiling, but less than in DOPC (Figure 6A). After boiling (Figure 6B), the FET efficiency in $C_{12}E_8$ increased to levels similar to those observed in DOPC vesicles. This indicates that donor and acceptor nonmixing in SDS and complete mixing in DOPC is not due to the presence of $C_{12}E_8$ in the labeled PLB stock solution. Also, the complete lack of energy transfer in SDS and less energy transfer in $C_{12}E_8$ before boiling indicates that there is no energy transfer between monomers or between pentamers of only donor and only acceptor.

Effect of Ca-ATPase on FET between PLB Subunits in DOPC. PLB and the Ca-ATPase were coreconstituted in DOPC membranes according to method I. FET was measured after reconstitution of equimolar ratios ($P_a = 0.5$) of two separate populations of donor- and acceptor-labeled PLB with varying molar ratios of the purified skeletal SR Ca-ATPase. The Ca-ATPase decreased E progressively as the ratio of Ca-ATPase to PLB was increased (Figure 7). The Ca-ATPase decreased the donor fluorescence slightly (3−4%) in the absence of acceptor, and this was taken into account when the energy transfer due to the acceptor was calculated. This correction did not have a significant effect on the conclusions.

The fluorescence energy transfer efficiency (E) was measured as a function of the molar fraction of acceptor at a molar ratio of 1.0 Ca-ATPase/PLB, using the two methods of coreconstitution that are described above. In method I (Figure 8A) in the absence of Ca-ATPase, the FET efficiency was similar to the results in Figure 5, giving a best fit to $n = 9-11$, with 12.6% ± 1.9% monomer, and an intersubunit distance $R = 8.2 \pm 0.1$ Å. In the presence of Ca-ATPase, energy transfer decreased substantially, giving a best fit of $n = 5-7$, with 35.1% ± 4.4% monomer, and an intersubunit distance $R = 20.3 \pm 2.1$ Å. These results indicate that interaction of PLB with Ca-ATPase not only partially depolymerizes the PLB oligomer but also increases the intersubunit distance R. FET results of method II (Figure 8B) in the absence of Ca-ATPase were essentially similar to those of method I, giving a best fit of $n = 9-11$, with 15.0% ± 4.3% monomer, and an intersubunit distance $R = 12.1 \pm 3.8$ Å. However, the data from method II in the presence of Ca-ATPase are best fit to $n = 5-7$, with 27.8% ± 0.8% monomer, and an intersubunit distance $R = 20.6 \pm 1.5$ Å, indicating a lesser degree of depolymerization compared to method I. Essentially similar results obtained from two different methods of reconstitution indicate that

Table 1: Summary of FET Results[a]

	reconstituted in DOPC		coreconstituted with Ca-ATPase in DOPC			
			method I		method II	
	SDS	DOPC	−Ca-ATPase	+Ca-ATPase	−Ca-ATPase	+Ca-ATPase
oligomer size, *n* (range)[b]	5−7	9−11	9−11	5−7	9−11	5−7
monomer, *x* (%)[c]	53.72 ± 5.04	12.78 ± 2.05	12.62 ± 1.87	35.12 ± 4.35	13.32 ± 4.20	27.12 ± 1.38
distance,[d] *R* (Å)	22.02 ± 2.74	8.87 ± 0.56	8.22 ± 0.12	20.29 ± 2.13	12.09 ± 3.83	20.62 ± 1.46

[a] Fit results for FET efficiency (E) vs molar fraction of acceptor (P_a) of ASE- and DABCYL-PLB in SDS, DOPC, and reconstituted in the absence and presence of Ca-ATPase. [b] Best fits (minimum χ^2) were obtained for more than one oligomeric size (indicated as range) for each experiment ($n \geq 3$). [c] The monomer was mean ± SE from the best fits for different oligomeric sizes (within the indicated range) from three different experiments. [d] Distance, R, is reported as mean ± SE from the best fits to different oligomeric sizes from three different experiments.

the effects of Ca-ATPase on the oligomeric state of PLB are functionally significant.

DISCUSSION

Summary of Results. We developed a method to label PLB specifically at Lys 3, using succinimido esters of ASE (donor) and DABCYL (acceptor) followed by treatment with DTT. Fluorescence energy transfer (FET) was used to study the oligomeric state of PLB solubilized by SDS and $C_{12}E_8$ and in DOPC lipid vesicles reconstituted in the absence and presence of Ca-ATPase purified from skeletal SR. Fits of the FET data to a symmetric ring-shaped oligomer model are summarized in Table 1. The dependence of FET on the molar fraction of acceptor indicates that PLB is predominantly in an oligomeric state having five (SDS) or more (DOPC) subunits, in equilibrium with ∼12% (DOPC) to ∼53% (SDS) in a monomeric form, and that the distance between the dyes on adjacent PLB subunits is ≤2.0 nm. We have shown that the presence of Ca-ATPase in the membrane partially depolymerizes PLB, decreasing the average oligomeric size (n), increasing the monomeric fraction (X), and increasing the intersubunit distance (R).

Labeling Specificity. We found that sulfonyl chlorides of dansyl and DABSYL label PLB with a dye/PLB molar ratio of ≥2.0, because these dyes react irreversibly with the side chains of Cys and Tyr, as well as Lys. The more amino-specific dyes, succinimido esters of ASE and DABCYL, reacted with these same side chains, but the labeling of Cys and Tyr side chains was reversed by treatment with DTT (Figure 2), hydroxylamine, or β-mercaptoethanol. Labeling PLB with ASE or DABCYL succinimido esters, followed by DTT treatment, yielded a dye/PLB molar ratio of 0.9−1.2, indicating specific and almost complete labeling of Lys 3.

PLB FET in Detergent Solution. For FET to occur within PLB oligomers, the mixing of two populations, randomizing the positions of donor-labeled and acceptor-labeled PLB in the oligomers, is a prerequisite. In SDS solution no energy transfer occurred, even after incubation for several hours, unless the sample was boiled after mixing (Figure 5). The SDS concentration (0.1%, 3.5 mM) was less than the critical micelle concentration (8 mM) so the lack of FET was probably not due to the presence of stable micelles. We conclude that PLB oligomers solvated by SDS are stable and do not dissociate into monomers and reassociate on the time scale of several hours at 25 °C. The fraction of monomer from FET (∼50%, Figure 5, Table 1) is much greater than observed on SDS−PAGE (∼20%, Figure 3). It is possible that the SDS−PAGE results are more reliable than our FET results in solution, since SDS−PAGE has the advantage of direct visualization. However, SDS−PAGE has the disadvantage of not having well-defined equilibrium conditions, as indicated by the wide variation in oligomer/monomer equilibrium on SDS−PAGE as a function of the concentration of SDS in the sample buffer, the time between boiling and loading the sample onto the gel, and the concentration of acrylamide in the gel (*1*, *30*). Thus, the oligomeric state on SDS−PAGE is indeterminate compared to the FET experiments, which are conducted in a well-defined solution that is equilibriated. $C_{12}E_8$ does not produce such slow kinetics of mixing, since significant FET occurs without boiling (Figure 6A). Boiling did increase FET in $C_{12}E_8$, reaching a level of FET that was much greater than in SDS, with a very low monomeric fraction remaining (Figure 6B).

PLB FET in DOPC Vesicles. After reconstituting dye-labeled PLB into DOPC bilayers, no boiling was required for FET to occur between donor- and acceptor-labeled subunits. This indicates that PLB molecules are in a dynamic equlibrum between monomer and oligomer in DOPC, which allows subunit mixing and exchange. Alternatively, this mixing and exchange could be occurring during the process of reconstitution, when PLB is in mixed micelles of detergent and lipid. Data analysis (Table 1) indicates that the high efficiency of FET in DOPC, compared with SDS, is due to an increase in average oligomeric size (9−11 vs 5−7), a decrease in the monomeric fraction (∼13% vs ∼53%), and a shorter intersubunit distance in the oligomer (∼9 Å vs ∼22 Å).

Attenuated total reflection Fourier transform infrared studies on PLB in supported lipid bilayers have indicated an angle of 50−70° between the cytoplasmic helix and the membrane normal (*28*). Assuming the length of the cytoplasmic helix to be 12−13 residues [residues 7−20 were estimated to be helical, on the basis of the Chou−Fasman method (*28*)], the distance between the N-terminal residues of helices in adjacent subunits would be in the range of 20−30 Å. In our FET experiments, the detected distance R between the donor and acceptor labeled on Lys 3 was 9 Å in DOPC and 22 Å in SDS. The value in SDS is in the lower end of the predicted range, while that in DOPC is smaller. Therefore, it seems most likely that the labels extend inward, toward the center of the oligomeric complex, as depicted in Figure 9. The shorter intersubunit distance observed in DOPC (9 Å) compared to SDS (22 Å) suggests that the cytoplasmic domains are tilted more from the vertical in SDS than in DOPC (Figure 9). This might be due to the different surface charge of the lipid and SDS: the positively charged cytoplasmic domains would be attracted by the surrounding

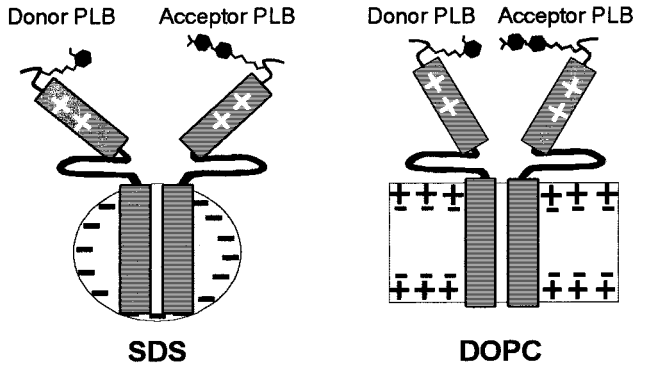

FIGURE 9: Model of PLB in SDS and DOPC showing the labels on Lys 3 facing the inside of the cytoplasmic domains in an oligomer (shown here as a dimer for simplicity). See text for discussion.

negatively charged SDS more than by the zwitterionic DOPC. Of course, Figure 9 shows just one of many possible models. For example, it is likely that PLB is flexible, so that there is not one well-defined distance *R* between the subunits. In that case, due to the R^{-6} dependence of FET, the average distance *R* would be underestimated.

Our value of 9−11 subunits per oligomer in DOPC, obtained from FET, is much higher than the 5 subunits expected on the basis of SDS−PAGE and confirmed by FET in SDS solution. This could be due to large oligomers having a specific size on the order of a decamer, but it seems more likely that it is due to the association of pentamers into larger aggregates.

PLB FET in DOPC Vesicles Reconstituted with Ca-ATPase. When labeled PLB was reconstituted with purified Ca-ATPase in DOPC vesicles, there was a gradual decrease in FET efficiency as the molar ratio of PLB/Ca-ATPase decreased (increasing concentrations of Ca-ATPase, Figure 7). At a PLB/Ca-ATPase molar ratio of 1.0 (Figure 8), data analysis showed that there is an increase in the fraction of monomer from 12−13% (method I − method II) to 27−35%, a decrease in the average oligomeric size from 9−11 to 5−7, and an increase in the intersubunit distance from 8−12 Å to 20 Å (Table 1). In method II, the results are similar to those obtained from method I, except that the fraction of monomer is less (27% vs 35%). These results indicate that the Ca-ATPase depolymerizes PLB oligomers into monomers and smaller oligomers (Figure 9). By use of site-directed mutagenesis followed by coexpression of PLB with SERCA2a, it has been shown that mutations that make PLB monomeric on SDS−PAGE are more potent inhibitors of Ca-ATPase (*14*, *15*). Our FET results of depolymerization of PLB in the presence of Ca-ATPase are consistent with the notion that the Ca-ATPase binds preferentially to the monomeric form of PLB (Figure 10), which acts as the most effective inhibitory species. This is also consistent with the hypothesis that depolymerization of PLB is an essential step for its inhibition of Ca-ATPase (*29*). Although the Ca-ATPase-induced increase in the monomeric fraction *X* can easily be explained by interaction between Ca-ATPase and PLB monomers, the substantial changes in *n* and *R* suggest strongly that the Ca-ATPase interacts directly with oligomers as well as monomers.

It is likely that the active inhibitory species of PLB is a monomer or an oligomer that is much smaller than the

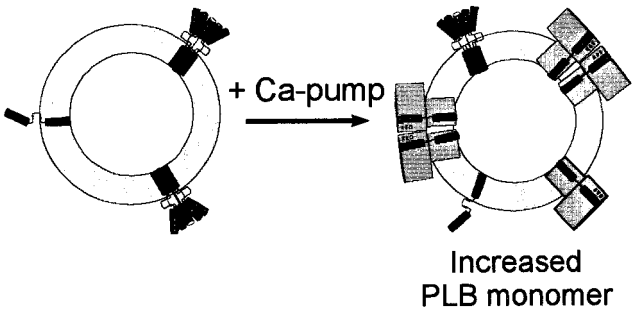

FIGURE 10: Effect of Ca-pump on the oligomeric state of PLB in DOPC vesicles. The fraction of monomeric PLB increases, suggesting that the pump associates preferentially with monomeric PLB.

average oligomer observed in the absence of Ca-ATPase. Our data indicates 27−35% of PLB monomer in the presence of equimolar amounts of Ca-ATPase, which represents an increase of 15−20% in the fraction monomer. This is comparable to the fractional inhibition observed at this level of PLB/Ca-ATPase (*17*), so it is possible that most or all of the inhibition is from PLB monomers. Given the experimental uncertainties involved, we cannot rule out the possibility that oligomeric PLB can also bind and inhibit the Ca-ATPase.

Conclusions. This study shows that fluorescence energy transfer is very effective in measuring the oligomeric state of PLB in lipid vesicles. The FET results showed the following: (a) PLB exists as a mixture of oligomer and monomer in both SDS solution and DOPC bilayers. The average oligomer size and molar fraction of monomer observed on SDS−PAGE is different from those in either an equilibrated SDS solution or a DOPC bilayer. (b) The average intersubunit distance in PLB at Lys-3 is ∼20 Å in SDS and ∼10 Å in DOPC: this small *R* suggests that the dye molecules are facing each other from inside the helical bundle. (c) Interaction of Ca-ATPase results in depolymerization of PLB into monomer and smaller oligomers, indicating that the Ca-ATPase binds preferentially to monomeric PLB but also interacts with oligomeric PLB and changes its structure.

ACKNOWLEDGMENT

We thank Roberta Bennett for help in fitting the fluorescence energy transfer efficiency data using a program she developed.

REFERENCES

1. Simmerman, H. K. B., and Jones, L. R. (1998) *Physiol. Rev.*, 921−947.
2. Colyer, J. (1993) *Cardiovasc. Res. 27*, 1766−1771.
3. Stokes, D. L. (1997) *Curr. Opin. Struct. Biol. 7*, 550−556.
4. Lindemann, J. P., Jones, L. R., Hathaway, D. R., Henry, B. G., and Watanabe, A. M. (1983) *J. Biol. Chem. 258*, 464−471.
5. Wegener, A. D., Simmerman, H. K. B., Lindemann, J. P., and Jones, L. R. (1989) *J. Biol. Chem. 264*, 11468−11474.
6. Luo, W., Grupp, I. L., Harrer, J., Ponniah, S., Grupp, G., Duffy, J. J., Doetschman, T., and Kranias, E. G. (1994) *Circ. Res. 75*, 401−409.
7. Wegener, A. D and Jones, L. R. (1984) *J. Biol. Chem. 259*, 1834−1841.
8. Watanabe, Y., Kijima, Y., Kadoma, M., Tada, M., and Takagi, T. (1991) *J. Biochem. (Tokyo) 110*, 40−45.

9. Simmerman, H. K. B., Kobayashi, Y. M., Autry, J. M., and Jones, L. R. (1996) *J. Biol. Chem. 271*, 5941−5946.
10. Arkin, I. T., Rothman, M., Ludlam, C. F. C., Aimoto, S., Engelman, D. M., Rothschild, K. J., and Smith, S. O. (1995) *J. Mol. Biol. 248*, 824−834.
11. Thomas, D. D., Reddy, L. G., Karim, C. B., Li, M., Cornea, R., Autry, J. M., Jones, L. R., and Stamm, J. (1998) *Ann. N.Y. Acad. Sci. 853*, 186−195.
12. Arkin, I. T., Adams, P. D., MacKenzie, K. R., Lemmon, M. A., Brunger, A. T., and Engelman, D. M. (1994) *EMBO J. 13*, 4757−4764.
13. Karim, C. B., Stamm, J. D., Joseph M. Autry, J. M., Thomas, D. D., and Jones, L. R. (1999), *Biochemistry* (in press).
14. Autry, J. M., and Jones, L. R. (1997) *J. Biol. Chem. 272*, 15872−15880.
15. Kimura, Y., Kurzydlowski, K., Tada, M., and MacLennan, D. H. (1997) *J. Biol. Chem. 272*, 15061−15064.
16. Cornea, R. L., Jones, L. R., Autry, J. M., and Thomas, D. D. (1997) *Biochemistry 36*, 2960−2967.
17. Reddy, L. G., Jones, L. R., Cala, S. E., O'Brian, J. J., Tatulian, S. A., and Stokes, D. L. (1995) *J. Biol. Chem. 270*, 9390−9397.
18. Schaffner, W., and Weissman, C. (1973) *Anal. Biochem. 56*, 502−514.
19. Stokes, D. L., and Green, N. M (1990) *Biophys. J. 57*, 1−14.
20. Reddy, G. L., Jones, L. R., Pace, R. C., and Stokes, D. L. (1996) *J. Biol. Chem. 271*, 14964−14970.
21. Levy, D., Bluzart, A., Seigneuret, M., and Rigaud, J.-L. (1990) *Biochim. Biophys. Acta 1025*, 179−190.
22. Levy, D., Gulik, A., Seigneuret, M., and Rigaud, J.-L. (1990) *Biochemistry 29*, 9480−9488.
23. Levy, D., Gulik, A., Bluzart, A., and Rigaud, J.-L. (1992) *Biochim. Biophys. Acta 1107*, 283−298.
24. Lanzetta, P. A., Alvarez, L. J., Reinach, P. S., and Candia, O. A. (1979) *Anal. Biochem. 100*, 95−97.
25. Chen, C. F. (1966) *Nature 209*, 69.
26. Cantor, C. R, and Schimmel, P. R. (1980) *Biophysical Chemistry*, Part II, p 451, Freeman and Company, San Francisco, CA.
27. Li, M., Reddy, G. L., Bennett, R. D., Silva, N. D., Jr., Jones, L. R., and Thomas, D. D. (1999) *Biophys. J.* (in press).
28. Tatulian, S. A., Jones, L. R., Reddy, L. G., Stokes, D. L., and Tamm, L. K. (1995) *Biochemistry, 34*, 4448−4456.
29. Kimura, Y., Asahi, M., Kurzydlowski, K., Tada, M., and MacLennan, D. H. (1998) *J. Biol. Chem. 273*, 14238−14241.
30. Reddy, L. G., Autry, J. M, Jones, L. R., and Thomas, D. D (1999) *J. Biol. Chem.* (in press).

BI981795D